

# Fingering instabilities of a reactive micellar interface

Thomas Podgorski<sup>1,2</sup>, Michael C. Sostarecz<sup>1</sup>, Sylvain Zorman<sup>2</sup>, and Andrew Belmonte<sup>1</sup>

<sup>1</sup>W. G. Pritchard Laboratories, Department of Mathematics,  
Penn State University, University Park, PA 16802, USA

<sup>2</sup>Laboratoire de Spectrométrie Physique,  
CNRS/Université Joseph Fourier, Grenoble,  
38402 Saint Martin d'Hères, FRANCE

(Dated: March 28, 2007)

We present an experimental study of the fingering patterns in a Hele-Shaw cell, occurring when a gel-like material forms at the interface between aqueous solutions of a cationic surfactant (cetyltrimethylammonium bromide) and an organic salt (salicylic acid), two solutions known to form a highly elastic worm-like micellar uid when mixed homogeneously. A variety of fingering instabilities are observed, depending on the velocity of the front (the injection rate), and on which uid is injected into which. We have found a regime of non-condensed stationary or wavy fingers for which width selection seems to occur without the presence of bounding walls, unlike the Saffman-Taylor experiment. Qualitatively, some of our observations share common mechanism with instabilities of cooling lava flows or growing biofilms.

PACS numbers: 83.60.Wc, 47.20.Gv, 83.80.Jx, 47.20.Ma

## I. INTRODUCTION

The classic instability of hydrodynamic fingering occurs when a uid of a certain viscosity is injected into a more viscous uid between closely-spaced parallel plates [1]; this Saffman-Taylor instability [2] has been widely studied, and has had many variants, including fingering in polymer uids, foams and gels [3, 4, 5, 6, 8]. The morphology of the instability can also be influenced by anisotropy [7], or modifications of the surface tension or density contrast between uids due to a chemical reaction [9, 10]. Hydrodynamic fingering is one of a wider class of instabilities occurring when one material is injected into another, or grows from a chemical or biological process; other such systems include smoldering flame fronts [11], lamellar microorganisms [12], silica or iron tubes forming around metal salt solutions [13, 14], growing biofilms [15, 16], or lava flows [17]. In many of these cases, the interface itself is defined by a reaction or a solidification which changes the material properties, and is driven by the expanding growth of the interior. The patterns in these systems result from a complex interaction of reaction, diffusion and mechanical effects in association with a particular rheology or elasticity of the interfacial zone.

Here we present a new type of pattern-forming instability, where fingering is linked to a rheological change – a gelling – due to a reaction which produces a viscoelastic micellar medium at the interface between two uids of identical viscosities in a Hele-Shaw cell [18]. The micellar gel-like medium is formed by reaction-diffusion at the in-

terface between two otherwise ordinary, water-like Newtonian uids of identical viscosities. One distinguishing aspect of our system is that the fingering occurs independent of which uid is injected into which, making this a true interfacial instability. In this paper we present our first exploration of this instability by varying uid characteristics (concentrations) as well as the flow rate.

The uids we study are aqueous solutions of the cationic surfactant cetyltrimethylammonium bromide (CTAB), and the organic salt sodium salicylate (NaSal), which form a strongly viscoelastic micellar material when brought into contact. It is well known that a viscoelastic uid is produced by the assembly of surfactants into long worm-like micelles, driven at low volume fractions by the mediating presence of certain slightly hydrophobic organic counterions [19, 20]. The essential difference between these worm-like micellar uids and more standard polymer uids is that these aggregates are in a dynamic equilibrium with free surfactants in solution due to breaking and reforming processes [21].

Much of the work on worm-like micellar uids has focused on their unusual properties, either rheologically [22, 23, 24, 25] or hydrodynamically [26, 27, 28, 29]; there has been less study of the reaction process between the surfactant and the salt which gives rise to the worm-like micelles [30]. In fact, the simple act of preparing these uids presents a startling phenomenon: two dilute solutions with essentially the physical properties of water become, upon combination, a strongly elastic uid.

## II. EXPERIMENTAL SETUP

The experiment consists of injecting one of the solutions into a Hele-Shaw cell previously filled with the other solution. Two cells were used in two different laboratories. Cell 1 (PSU) is made of two 9.5 mm-thick square

Present address: Dept. of Physics, Monmouth College, Monmouth, IL.

<sup>2</sup>Also at Harvard School of Engineering & Applied Sciences, Harvard University, Cambridge, MA.

glass plates, 15 cm  $\times$  15 cm. Cell 2 (UJF) is made of two 10 mm thick glass disks, 20 cm in diameter. A gap  $b = 0.6$  mm between the two plates is fixed by brass shims. A light box below the cell provided a nearly uniform illumination (light box from Schott-Fostec for cell 1, a4 electro-luminescent panel from Selectronic for cell 2), and the pattern growth is observed from above by a COHU 4912 video camera connected to a Macintosh computer.

In most experiments, the cell is initially filled with a solution of NaSal (Sigma-Aldrich) of a given concentration. A small amount of blue McCormick or green (Vahine) food coloring is added to this solution for purposes of visualization. The injected surfactant solution (CTAB, Sigma-Aldrich) is uncolored. In all experiments, both solutions have the same concentration, ranging from 25 to 50 mM. Injection is made through plastic tubing at the center of the top plate of the Hele-Shaw cell by a KD S100 syringe pump at a constant flow rate  $Q$ , which ranges from 0 to 1000  $\mu$ l/h (0.278 ml/s). In some experiments, the opposite arrangement of fluids was tested: NaSal solution injected into CTAB.

Two kinds of experiments were run: i) radial injection experiments, where the fluid is injected in an axisymmetric fashion in the Hele-Shaw cell, and ii) linear experiments where the initial direction of flow was imposed thanks to a U-shaped shim placed around the injection hole, aimed at studying isolated fingers.

### III. EXPERIMENTAL RESULTS

#### A. Radial geometry

The two solutions of CTAB and NaSal, at equimolar concentrations ranging from 25 to 50 mM are completely Newtonian before they are brought into contact with each other, each with a viscosity indistinguishable from that of pure water. Consequently, in the absence of the "worm-like micellar reaction" at the interface, a Saman-Taylor experiment would exhibit a completely stable radially expanding circle. Instead, as the front moves away from the injection point and the injected volume increases, a sequence of growth regimes takes place.

We begin by discussing the injection of the surfactant solution (CTAB) into the solution with the organic counter-ion (NaSal). A stable circular expansion is observed in our experiment at high injection speeds, which occur close to the injection point due to the constant flow-rate condition. In that case, when the radius  $R$  of the expanding CTAB solution is small, or equivalently when the speed  $dR/dt$  is large, the gelling reaction occurs at a slower timescale than the stretch rate of the gelled membrane which remains thin and offers no resistance to flow: the boundary between fluids is stable and isotropic. The gel at the interface is probably very thin and dilute, and does not break or split (Fig. 1a).

When  $R$  reaches some critical value which depends

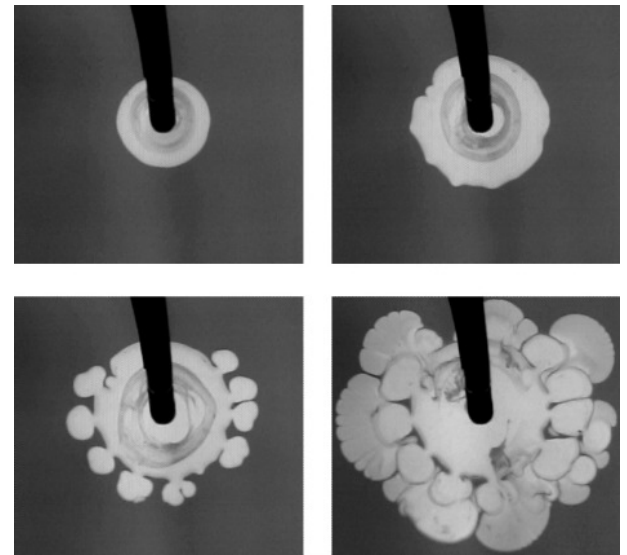


FIG. 1: The onset of the fingering instability for an expanding circular front driven by an injection rate of 150  $\mu$ l/hr, 30 mM CTAB solution injected into 30 mM NaSal solution:  $t = 10.0$  s,  $t = 20.0$  s,  $t = 28.8$  s,  $t = 64.7$  s. Scale: picture width is 8 cm.

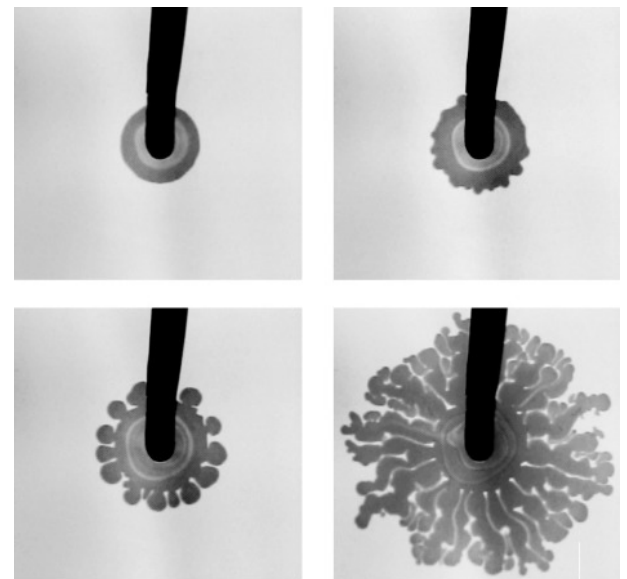


FIG. 2: Fingering instability under the same conditions as Fig. 1, but with the opposite arrangement of fluids - 30 mM NaSal solution injected into 30 mM CTAB solution:  $t = 8.2$  s,  $t = 11.0$  s,  $t = 16.3$  s,  $t = 54.8$  s. Scale: picture width is 8 cm

on flow-rate and concentrations, perturbations are observed on the smooth front (Fig. 1b). The result of this instability is that the constant flow rate  $Q$  focuses into the perturbations, which become more "active" and bulge out into mushroom shapes. Meanwhile, the regions between the bulges slow down, and appear to harden. Subsequently, each individual mushroom spreads almost

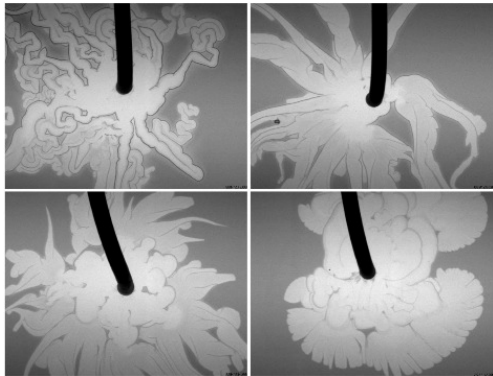


FIG. 3: Fingering patterns for different flow rates after the same total volume ( $4 \text{ ml}$ ) of  $50 \text{ mM}$  CTAB has been injected into  $50 \text{ mM}$  NaSal: a)  $20 \text{ ml/h}$ ; b)  $50 \text{ ml/h}$ ; c)  $100 \text{ ml/h}$ ; d)  $200 \text{ ml/h}$ . The dark borders are the gelled interfaces, which bound the interior, owing conduit of fresh uid which drives the further growth of the pattern.

isotropically, albeit at a slower rate than the initial front, as each is effectively fed with a reduced flow rate (e.g. about  $Q=10$  in Fig. 1c). The appearance of these mushroom shapes around the perimeter bear a striking resemblance to the "breakout" of a lava flow [17].

A precise determination of the onset of the first instability leading to the mushroom pattern can be made by measuring the radius of the circle circumscribing the growing front as a function of time; when the circular front becomes unstable to fingerlike protrusions, the growth rate of the gel front (and the entire pattern) goes through a rapid increase. We find an initial quantitative agreement with the constant flow rate law  $R(t) = \sqrt{Q}t = b$ , where  $Q$  is the imposed flow rate and  $b$  is the gap width. As the gel front slows, an instability appears nearly simultaneously around the circular front. These perturbations grow, and take on the appearance of mushrooms, as shown in Fig. 1. These new fronts, which have focused the flow from the center, move at a faster rate than the front just before the instability. Eventually these fronts slow down as the pattern expands in size, and a second generation of fingers breaks from the pattern.

Surprisingly, we observe the same instability to the mushroom pattern by performing the inverse experiment: injecting a  $30 \text{ mM}$  NaSal solution at the same rate into a  $30 \text{ mM}$  CTAB solution (Figure 2). The fact that the instability occurs independent of which uid is injected into which distinguishes this from Saffman-Taylor and other related fingering instabilities, and shows that this fingering is truly driven by an interfacial instability. Nevertheless, the critical radius at which the circular front becomes unstable is significantly smaller as can be seen when comparing Figures 1 and 2. This may be due to different diffusion coefficients of CTAB and Salicylate, or different compositions of the micellar media formed when injecting the surfactant into the salt or the opposite arrangement.

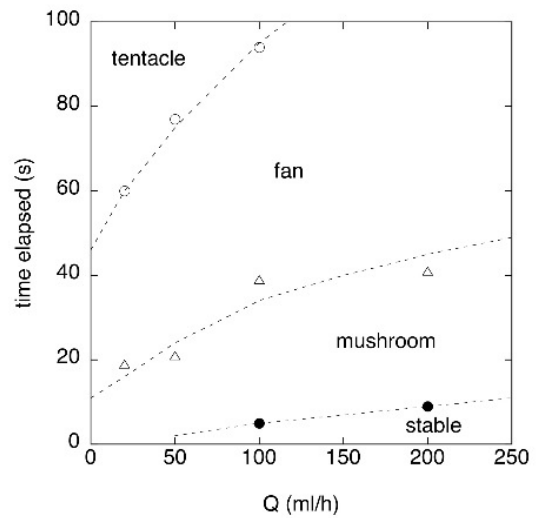


FIG. 4: Phase diagram for the injection of  $50 \text{ mM}$  CTAB into  $50 \text{ mM}$  NaSal: Time at which successive regimes are triggered vs. flow rate.

In the mushroom instability, the interfacial membrane between the two solutions appears to break simultaneously at a number of points along the perimeter. Bulges of uid protrude, and the gel-like material forms at the new interfaces. When this becomes more solid, it resists further smooth growth, but under the imposed conditions of constant injection rate, the pressure of the internal uid will increase until a rupture of the gel membrane occurs again, and the process of fingering repeats.

Close observation of the interface between the two uids reveals that the membrane is thickening with time, evidently due to the further reaction of surfactant and organic counterion diffusing through the material already formed. This thickening is made obvious by the slightly darker color of the material at the interface. It has also been confirmed by a post-mortem test after the experiment: when the glass plates are separated, that the darker material is indeed gel-like, and clings to the glass while the two uids rapidly flow away as the cell is emptied. This is most likely the reason that the membrane elasticity and resistance to flow increase with time. When some material threshold is reached [31], a fracture occurs in the membrane and fresh uid leaks and forms the next generation of mushrooms. However, the relatively well-defined wavelength of the mushroom pattern and the simultaneity of finger appearance suggests an underlying mechanism based on gel characteristics (thickness, concentration) prior to fracture.

Note that the subsequent evolution of the patterns in Figs. 1 and 2 differs for the two injection arrangements: while the experiment injecting CTAB solution into NaSal solution leads to other instabilities (described next), the other arrangement is simpler. The same process of expansion, hardening, fracture, and break-out seems to repeat as the pattern expands, without any other mor-

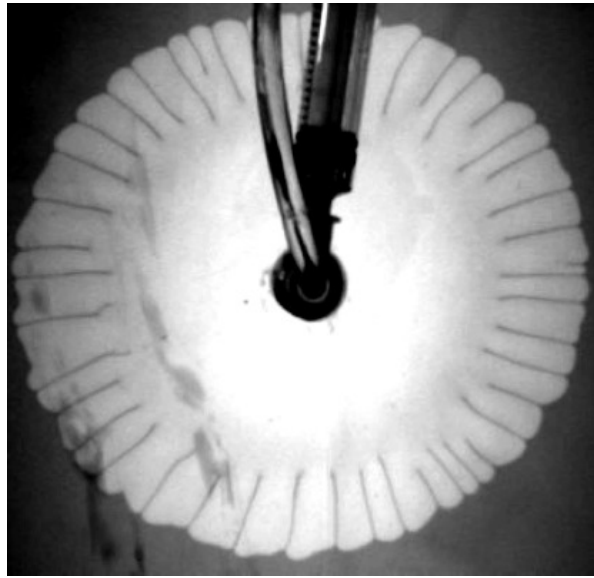


FIG. 5: A regular pattern of fingers in the fan state, obtained when injecting 35 mM CTA B into 35 mM NaSal,  $Q = 600$  ml/hr. Scale: picture width is 10 cm.

photogies.

We have identified two other instabilities which occur at later times as the radial pattern expands. After a few generations of mushroom patterns, we observe a transition to a fan-like pattern of contiguous wide fingers, giving the growing front a sort of flower-like appearance. The fingers emerging from these fans eventually become narrower 'tentacles', which then undergo a curling instability and start to meander. These tentacles seem to prefer growing along an existing structure rather than into fresh uid. By changing the injection rate  $Q$ , the different growth regimes can be shifted both radially and in time: at higher injection rate, a given pattern instability is found to occur at larger distances from the center while at lower flow rates, the isotropic regime is almost invisible and the first observed pattern can be mushroom s or even multiple tentacles diverging from the injection point (see fig. 3). The way this sequence of instabilities and patterns takes place as a function of flow rate is summarized in the schematic phase diagram of fig. 4 for 50 mM concentrations.

While some regimes can be skipped by lowering the flow rate, which effectively shrinks patterns radially down to the center, there are also ranges of concentrations and flow rates for which the fan instability is the first one to occur, directly after a stable circular front has grown to a finite distance from the center, as shown in Fig. 5 for  $Q = 600$  ml/h and 35 mM concentration.

The second pattern observed in this experiment ('fans') clearly involves an instability with a well defined wavelength (figs. 3(d) and 5); while it appears to be similar to the first instability, the wavelength is much smaller. This underlines a major influence of the radial expansion: a consequence of interface elongation is an az-

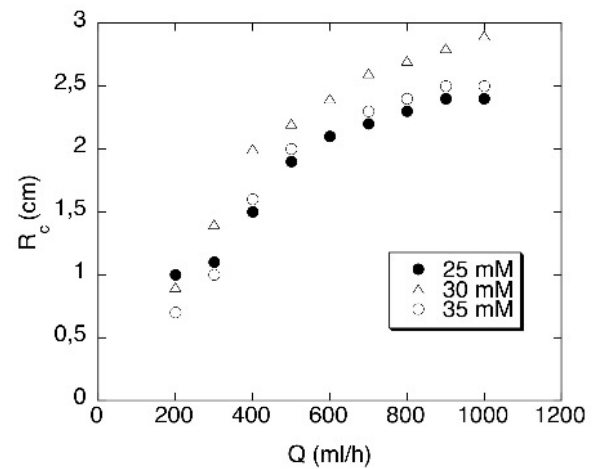


FIG. 6: Critical radius of breakdown of axial symmetry vs. flow rate for three different CTA B / NaSal concentrations.

imuthal tension in the gel membrane which stabilizes the shortest wavelengths, in a similar fashion to surface tension in the classic Saffman-Taylor instability [1]. As the radius of the injected uid increases, membrane stretch rate decreases and the interface destabilizes.

More quantitative data on the onset of the first instability seen after the stable circular growth was obtained from the conditions when the stable circular growth stops and either a regular array of fingers characteristic of the fan state (as in Fig. 5), or a mushroom pattern (as in Fig. 1) appears. Figure 6 shows the evolution of the critical radius at which the axial symmetry is lost vs. flow rate for three different concentrations. The critical radius increases with the flow rate: the gel membrane stretch rate being higher, it takes longer to become thick enough and trigger the instability. As far as concentration is concerned, one would intuitively expect that the stronger the concentration, the harder the gel. Thus the gel breaking should occur sooner for higher concentrations. However, an inversion is seen in Fig. 6: the curve for 25 mM is below others at high flow rate. This might be due to a different rheology at different concentrations (e.g. shear thinning occurring at different shear rates).

The evolution of fingers in the tentacle state (Fig. 7) is significantly different than either the mushroom or fan state: the growth is very localized at the tip. The freshest uid arrives at the tip from the interior of the finger, where it has not yet hardened to an immobile state, and is advected to the sides by the feeding flow, where the interface solidifies. We expect this instability to occur when the rate of creation of new interface exceeds the hardening time of the gel.

A remarkable feature of these tentacles is their roughly constant width. Since in this regime the average number of tentacles is typically constant (see Fig. 8, which appears to have reached a steady state of 11 fingers), the velocity of the moving tip must on average also be

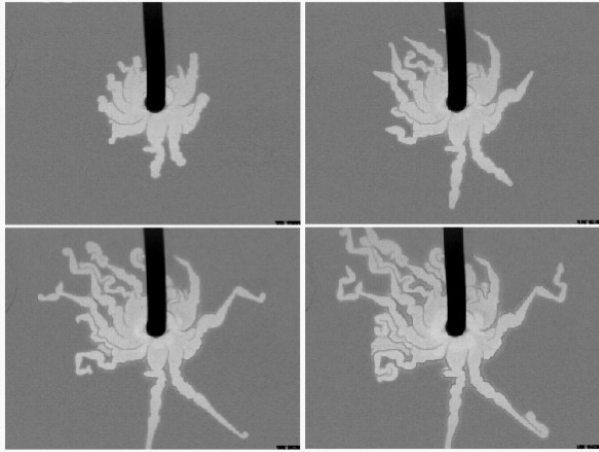


FIG . 7: Growth of the micellar gel pattern in the tentacle state, for the injection of a 50 mM CTA B solution into a 50 mM NaSal solution, at a flow rate  $Q = 20 \text{ ml/h}$ . The width of each image is 11 cm .

constant. Tentacles can therefore be seen as a state to which the system is attracted under certain conditions are reached: critical width (or wavelength of the 'fan' instability) and critical velocity.

The stability of this regime can be qualitatively explained in the following way: a slight decrease of the nger width leads to a velocity increase because of the constant flow rate. The gel at the tip would then be weaker, which favors radial growth and tip widening. Conversely, a slight increase in nger width would decrease the nger velocity, which would give more time for the gel to harden. This would result in a greater resistance to nger widening. Gel fracture would then occur and redirect the flow. We focus on this nger regime in next section.

Curling structures appearing in the ultimate developments of tentacle growth, the tip favors motion along an existing membrane. One mechanism for this could be that in these regions a depletion of the outer solution (NaSal) has occurred. As a consequence, the gel forming there is weaker and poses less resistance to flow, resulting in an effective attraction between growing ngers.

### B . Linear geometry - single nger growth

While our initial observation of micellar interface ngering was made in a radial injection experiment, the geometry complicates the dynamics at a fixed flow rate, since the front speed decreases with radius as the pattern spreads out. We therefore performed a second series of experiments in a linear geometry at LSP in Grenoble.

In order to investigate the remarkable nger growth regimes seen in the ultimate stages of radial growth, we made experiments focused on the study of this particular pattern. A small device (U-shaped plate) was placed in the Hele-Shaw cell around the injection point to promote

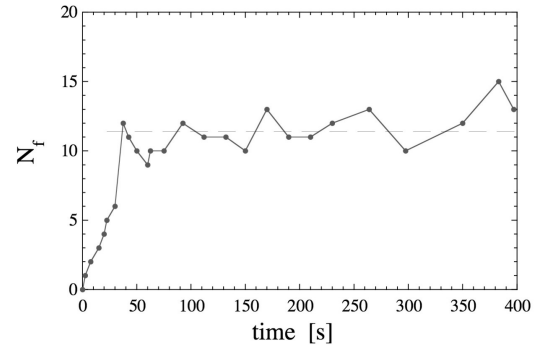


FIG . 8: The total number of actively growing ngers  $N_f$  in the tentacle growth state as a function of time (50 mM CTA B solution injected into 50 mM NaSal solution at 20 ml/hr).

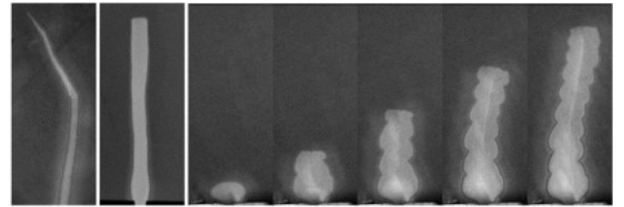


FIG . 9: Linear nger growth regimes. Left to right: evanescent nger (concentration  $c = 30 \text{ mM}$ , flow rate  $Q = 1 \text{ ml/h}$ ), steady nger ( $c = 40 \text{ mM}$ ,  $Q = 2.5 \text{ ml/h}$ ), wavy/oscillating nger growth ( $c = 30 \text{ mM}$ ,  $Q = 1.5 \text{ ml/h}$ ). Each picture is 2 cm wide, and the time interval between wavy nger pictures is 150 s.

single nger growth in a certain direction, allowing precise control of the flow rate inside the nger. The plate forms a small channel of width 3 mm and length about 2 cm . Note that this channel serves only to set the initial condition: nger growth is observed once the uid is coming out of the channel: the nger grows in an unconfined half-space. When the flow rate  $Q$  is in the correct range (approximately  $0.3 \text{ ml/h}$ ), a single nger grows. For  $Q > 3 \text{ ml/h}$ , it becomes unstable and splits into two or more ngers.

We observed different types of ngers, depending on flow rate and concentration see Fig. 9. For a given concentration, at low flow rates ngers are evanescent: their width decreases as the nger grows until the narrow tip opposes too much resistance to flow. Then the membrane breaks somewhere and a new evanescent nger grows. At intermediate flow rates (close to  $2 \text{ ml/h}$ ), there exists a narrow range where steady growth occurs: ngers keep a constant width and the front moves at constant speed. Above this range, one observes surprising oscillating ngers: the front periodically expands and contracts, modulating tip width.

Note that in both cases only the nger tip is active; the sides remain fixed, and only thicken slightly with time as discussed above. Another remarkable feature is the tip shape: it is a straight front, perpendicular to the direc-

tion of motion, except for evanescent fingers at the end of their life. This is completely unlike the rounded tips of most Saman-Taylor fingers, and also the needle-like fingers seen in fingering experiments on non-Newtonian associating polymer fluids [36] or colloidal pastes [37].

Moreover, the fact that the finger has a selected width while being far from any sidewalls is very different than the classic Saman-Taylor case or the fan state described above, where the finger width is half of the channel width (without surface tension effects) [1]; in a radial flow with far away boundaries the fingers expand and split [32, 33]. This difference is a consequence of the rapid formation of a gel-like membrane that poses a strong resistance to flow, preventing finger widening. We suspect that in evanescent fingers the pressure and velocity are too low to prevent quick widening of the gel membrane toward the inside of the finger. The oscillation mechanism in wavy fingers is more mysterious. The oscillation mechanism in wavy fingers is more mysterious. Given the fact that timescales involved in this process (~100 s) could be of the same order of magnitude as rheological times of the micellar fluid, it may share a common origin with the stick-slip instability suggested by Pu et al. [6], however a more detailed characterization of the material will be needed to test the connection.

#### IV. DISCUSSION AND CONCLUSIONS

We have presented here a new kind of fingering instability in a Hele-Shaw cell, defined by the interface between two solutions which together form worm-like micelles. The most striking aspect of these fingers is that the instability is completely determined by the properties of the interface. This is shown by the fact that essentially the same instability occurs independent of which solution is injected into which (in fact both solutions have the same viscosity). We have seen that there are some differences between these two patterns, which may arise from an asymmetry in diffusion coefficients of the two reacting species – it is very likely that the salicylate ion has a higher mobility in water than either a spherical micelle

or a single surfactant molecule.

To our knowledge, the complex morphology of a growing, gelling interface has not previously been studied; however the early work by Hatschek on the gelling of a sinking drop of reactive fluid during vortex formation is similar in spirit [34, 40]. From our observations, many physical processes seem to influence pattern formation in this system: reaction-diffusion, flow and rheology of the viscoelastic micellar gel. The instabilities of such a system provide a new set of mechanisms which are of potential relevance to processes occurring in the growth of biological structures like bacterial biofilms.

Although our system is not explicitly biological, it includes many physical aspects of biofilms, such as the formation and growth of an elastic gel subjected to flow. Our study sheds light on the purely physical instabilities to which such a system is susceptible. The general problem of an expanding or growing gel finds an important application in certain biomedical infections, where the bacteria secrete a resistant biofilm matrix, which supports and protects them, often against disinfectants and antibiotics; an important example is *Pseudomonas aeruginosa*, responsible for many hospital infections [38]. Our experimental results seem most closely related to other finger-like structures driven by dynamic growth or cooling processes, such as those produced by the rupture of the cooled crust of flowing lava [17]. While much remains to be done to reach a quantitative understanding, the experiment we present here shares common qualitative features with many of these systems, and could be seen as a representative reaction-diffusion-advection system, displaying similar pattern formation but in a more convenient to controlled laboratory study than infectious biofilms or flowing lava.

AB acknowledges discussions with M. Clayton and J. P. Keener, and support from the Alfred P. Sloan Foundation, and the National Science Foundation (CAREER Award DMR-0094167). TP and SZ wish to thank O. Pierre-Louis for helpful discussions and J. Schaperklaus for experimental help. TP also acknowledges financial support from DGA (French Ministry of Defense).

---

[1] Dynamics of Curved Fronts, P. Pelce, ed. (Academic Press, 1988).

[2] P. G. Saman & G. I. Taylor, Proc. Roy. Soc. London A 245, 312 (1958).

[3] Nittman, J., Daccord, G., & Stanley, H. E., Nature 314, 141 (1985).

[4] S. Park & D. Durian, Phys. Rev. Lett. 72, 3347 (1994).

[5] P. Fast, L. Kondic, M. J. Shelley, P. Palyy-Muhoray, Phys. Fluids 13 1191{1212 (2000).

[6] N. Pu, G. D. ebregas, J.-M. Di Meglio, D. Higgins, D. Bonn, C. Wagnier, Europhys. Lett. 58, 524 (2002).

[7] V. Horvath, T. V. Icsé, & J. Kertesz, Phys. Rev. A 35, 2353 (1987).

[8] A. Lindner, P. C. Cossot, & D. Bonn, Phys. Rev. Lett. 85, 314 (2000).

[9] A. Dewitt & G. M. Homsy, Phys. Fluids 11, 949{951 (1999).

[10] A. Dewitt, Phys. Rev. Lett. 87, 054502 (2001).

[11] O. Zik, Z. Olam, & E. Moses, Phys. Rev. Lett. 81, 3868 (1998).

[12] A. Gordey & M. Tabor, Phys. Rev. Lett. 90, 108101 (2003).

[13] S. Thouvenel-Romans & O. Steinbock, J. Amer. Chem. Soc. 125, 4338 (2003).

[14] D. Stone & R. E. Goldstein, Proc. Natl. Acad. Sci. 101, 11537 (2004).

[15] T. B. Reynolds & G. R. Fink, *Science* 291, 878 (2001).

[16] J. D. Ockery, I. K. Alper, *SIAM J. Appl. Math.* 62, 853-869 (2001).

[17] R. W. Grishuis, *Ann. Rev. Fluid Mech.* 32, 477-518 (2000).

[18] A. Belmonte, T. Podgorski, M. Sostarecz, & S. Zorman, *Bull. Am. Phys. Soc.* 50, GF.00006 (2005).

[19] H. Rehage & H. Homann, *Mon. Phys.* 74, 933 (1991).

[20] R. G. Larson, *The Structure and Rheology of Complex Fluids*, (Oxford, 1999).

[21] Israelachvili, J. *Intermolecular and Surface Forces*, 2nd edition, (Academic Press, 1991).

[22] T. Shikata & H. Hirata, *J. Non-Newtonian Fluid Mech.* 28, 171 (1988).

[23] C. Grand, J. Arnault, & M. Cates, *J. de Physique II* 7, 1071 (1997).

[24] S. Lerouge, J-P. D'ecruppe, J-F. Berret, *Langmuir* 16, 6464 (2000).

[25] C. Liu & D. Pine, *Phys. Rev. Lett.* 77, 2121 (1996).

[26] L. Smolka & A. Belmonte, *J. Non-Newtonian Fluid Mech.* 115, 1 (2003).

[27] N. Z. Handzy & A. Belmonte, *Phys. Rev. Lett.* 92, 124501(4) (2004).

[28] S. Chen, J. P. Rothstein, *J. Non-Newtonian Fluid Mech.* 116, 205-234 (2004).

[29] P. Ballesta, S. Manneville, *Phys. Rev. E* 71, 026308 (2005).

[30] Lin, Z., Cai, J. J., Scriven, L. E., D'avis, H. T. *J. Phys. Chem.* 98, 5984 (1994).

[31] J. R. G. Ladden & A. Belmonte, submitted to *Phys. Rev. Lett.*

[32] G. M. Homsy, *Ann. Rev. Fluid Mech.* 19, 271 (1987).

[33] L. Paterson, *J. Fluid Mech.* 113, 513 (1981).

[34] D. W. Thompson, *On Growth and Form*, (Cambridge, 1942); Ch. 5, 'The Forms of Cells'.

[35] M. E. Cates & S. J. Candau, *J. Phys.: Condens. Matter* 2, 6869 (1990).

[36] J. Ignes-Mullol, H. Zhao, & J. V. Maher, *Phys. Rev. E* 51, 1338 (1995).

[37] E. Lemaire, P. Levitz, G. D'Accord, & H. Van Damme, *Phys. Rev. Lett.* 67, 2009 (1991).

[38] J. W. Costerton, P. S. Stewart, & E. P. Greenberg, *Science* 284, 1318 (1999).

[39] O. Matar & S. Troian, *Phys. Fluids* 11, 3232 (1999).

[40] E. Hatschek, *Proc. Roy. Soc. London A* 95, 303 (1919).